Wrought Al - Cast Al compound casting based on zincate treatment for aluminum wrought alloy inserts

Matthias Schwankl*, Jonathan Wedler, Carolin Körner

Friedrich-Alexander University Erlangen-Nuremberg, Institute for Material Science, Chair of Materials Science and Engineering for Metals, Martensstraße 5, 91058 Erlangen, Germany

ABSTRACT

The surface properties of solid inserts are critical to the development of a reaction zone in compound castings. In contrast to prior works (based on Al99.5) the goal of this paper is to apply the zincate treatment to different aluminum wrought alloys. This enables the possibility to create compound structures with enhanced mechanical properties. During zincate treatment the aluminum oxide layers are dissolved and a thin layer of zinc (<500 nm) prevents reoxidation. Coating parameters are optimized especially for compound castings: maximum coverage of the surface and high coating adhesion implemented by double zincate treatment. The pretreated inserts are embedded in an aluminum component by high pressure die casting. A sound metallic bonding between both aluminum alloys develops due to diffusion and reaction zones. Mechanical tests confirm a sound metallic bonding. Depending on the integrated wrought alloy enhanced mechanical properties of the compound structure can be achieved. Microprobe and fracture analysis provide detailed information about the interface properties of the compound structure, which can be enhanced by thermal treatment.

1. Introduction

Combining different light metal alloys within one component without additional joining processes provides the possibility to implement specific properties at the points needed. In the last years compound casting (also referred to as Bi-metallic casting in the works of Zhang et al., 2014) has been in the focus of industrial as well as scientific research activities. Depending on the desired product, specific material combinations can be used. On the basis of aluminum different materials and methods are described in relevant publications. Al-Mg-, Al-Fe- and Al–Al-based compounds can contribute to lightweight designs to create an optimum of adapted strength and low density. The following compound examples demonstrate that especially with Al-Mg and Al-Fe problems occur with the formation of intermetallic phases (IMPs).

Papis (2009) showed in his dissertation that a wide range of technologies has been developed to join aluminum and magnesium. All authors reported the formation of intermetallic phases (IMPs). In order to prevent the formation of Al-Mg IMPs, a protective layer of manganese was applied to the Al substrate. It was observed that the formation of Al-Mg phases could be successfully prevented but still Al-Mn IMPs occurred leading to embrittlement.

Viala et al. (2002) investigated the IMP development between an Al-Si cast alloy and a cast iron insert. The interface layer – mostly AlFe-IMPs – was able to withstand moderate mechanical loads. Nevertheless, thermal treatment should be avoided. Reheating at 520 °C followed by water quenching led to increased diffusion of Al and the interface was drastically weakened by the formation of Kirkendall voids.

Papis et al. (2008) investigated Al–Al compound castings on a laboratory scale. Using the so-called "zincate treatment" an oxide-free surface coated with zinc could be fabricated which promoted wetting of the aluminum substrate material. Also and most importantly, those compound castings did not show any signs of IMP-development and therefore the mechanical properties of wrought alloys and the good castability of Al-cast alloys can be combined.

Due to these findings the zincate process was also used by Rübner et al. (2011) and Liu et al. (2015) in combination with thicker (>1 μm) additional Zn-coatings to successfully manufacture compound castings based on hpdc- and squeeze casting technology, respectively. Compounds purely based on zincate coatings could not be realized due to fact that the coating was washed away into the casting matrix. Therefore cracks occurred at the interface.

* Corresponding author.
  E-mail addresses: Matthias.Schwankl@fau.de, m.schwankl@web.de
(M. Schwankl).

These results are contrary to the investigations made by Körner et al. (2014) in which the same experimental setup as described by Rübner et al. (2011) was used, except no additional zinc was applied by means of electrochemical methods. Solely for the fact that very thin zinc-coatings (<500 nm) enabled the formation of sound metallic interfaces for Al99.5/AlSi9Cu3 compound castings. Depending on the casting thickness and tool temperature a process window could be identified and verified for a plate-like casting.

In contrast to previous work, where pure Al-Inserts were used, the focus of this paper is on combining aluminum wrought and cast alloys. Because of the different electrochemical behavior of wrought alloys due to their varying content of alloying elements it is necessary to adapt the zincate treatment. In the first part the different coating behavior of Al-wrought alloys in contrast to Al99.5 is presented and explained. Furthermore, mechanical tests and microprobe analysis give a deep insight in the properties of the Al–Al-compound castings, manufactured by cold chamber high-pressure compound casting. Interestingly, the casting process itself influences the hardness of the wrought alloy insert because of the thermal influence on the insert during casting. Therefore the compound properties themselves are changed, which is explained due to the strengthening influence of the wrought alloys. Investigations of the fracture mechanisms conclude the work.

2. Materials and methods

2.1. Zincate process for Al wrought alloys

Three types of rolled wrought Al alloys were used as insert. The size of the insert was $100 \times 30 \times 1$ mm. Table 1 shows the compositions (DIN EN 573-3) and information about heat treatability, weldability and general advantages of the materials according to DIN EN 573-4, DIN EN 1011-4, Ostermann (2007) and Kammer (1998).

Wrought alloys can only contribute with their varying properties (see Fig. 1) if a sound bonding to the casting matrix can be realized. In the present work this is accomplished by etching the surface to dissolve the aluminum oxide barriers on the surface. The work of Hino et al. (2009) showed that reoxidation is prevented by simultaneously applying a very thin layer of Zn (<1 μm) to the surface of the aluminum wrought alloys. This was performed by means of a zincate treatment similar to that described in the work of Papis et al. (2008). Layers thicker than 10 μm lead to hot crack formation in the applied casting setup which was shown by Rübner et al. (2011).

As described in Schwankl et al. (2013), subsequent to removing organic and loose dirt particles, the surface was roughened by sandblasting with a SiC grit at 2 bar (medium grain size of 35.3–39.1 μm according to DIN ISO 8486-2). This was followed by cleaning the insert in an ultrasonic acetone bath for 15 min, rinsing with deionized water and dehumidifiying.

To get an oxide-free aluminum surface and to facilitate bonding of an aluminum insert to metallic melts during casting, a combination of different chemical reactions is necessary. The applied process steps are based on the research of Schwankl et al. (2013), in which the parameters prior to the coating (cleaning and sandblast-
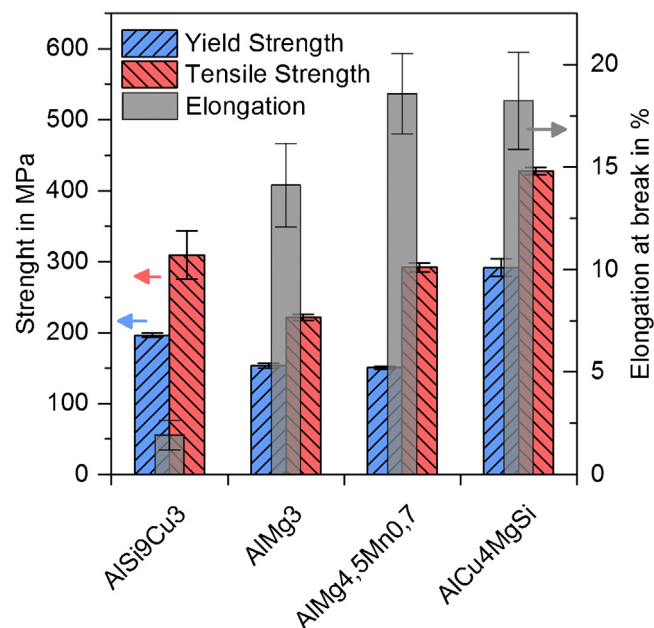

Fig. 1. Mechanical material properties for selected aluminum cast and wrought alloys applied in this work. Sample geometry and experimental setup according to DIN 50125.

ing with SiC) were in the focus of coating experiments. Different wrought alloys with different compositions of the natural oxide layer were used. Therefore it was essential to adapt the zincate treatment, the zincate solution and the process times. Fig. 2 shows the zincate treatment process which was used for the coating of AlCu4MgSi, AlMg4.5Mn0.7 and AlMg3 specimens.

Subsequently, sandblasting and cleaning of the surface was performed and mixed oxides were removed by immersing the inserts in a hydrofluoric-nitric-acid solution (4% HF and 50% HNO_3). When the surface was free of mixed oxides, a primary zinc layer was generated in the sodium-based zincate pickle. For the coating experiments itself the commercial zincate solution NICAL EA (*RIAG AG*) was used. In order to gain a high degree of coating and layer adhesion, the inserts were dipped in a 40% HNO_3 bath to partly remove the first zinc layer crystals. Jin et al. (2004) investigated the crystallisation mechanisms during the zincate process and according to his findings, the remaining Zn crystals act as nucleation sites for the second zincate coating step. To eliminate contamination among the chemicals, the inserts were rinsed with deionized water between each process step and dehumidified with a dryer. The chemical baths were agitated by magnetic stirrers.

Due to the varying composition of the aluminum alloys and oxide layers, a parameter study was performed for each investigated alloy according to Table 2. The starting parameter set "AP" was given by the supplier of the chemicals. Variations concerning dipping time for different process steps were carried out and were linked to the nomenclature in the first column of Table 2.

Table 1
Compositions, heat treatability, weldability and advantages of insert materials.

Notation		max. (in wight.-%)					Heat treatment	Weldability	Note
Numerical	Chemical	Si	Fe	Cu	Mn	Mg			
EN AW-2017A	AlCu4MgSi	0.2–0.8	0.7	3.5–4.5	0.4–1	0.4–1	artificial ageing	sufficient-difficult	very high strength
EN AW-5283A	AlMg4.5Mn0.7	0.3	0.3	0.3	0.5–1	4.5–5.1	natural hard	very good	highest strength of non ageable alloys
EN AW-5754	AlMg3	0.4	0.4	0.1	0.5	2.6–3.6			

Table 2
Process times of the zincate parameter study.

Sets of parameters	1) 4% HF 50% HNO$_3$	2) Zincate mordant	3) 40% HNO$_3$	4) Zincate mordant
AP	180 s	120 s	50 s	60 s
P1, P2, P3	60, 90, 120 s	120 s	50 s	60 s
P4, P5, P6	120 s	100, 150, 180 s	50 s	60 s
P7, P8, P9	120 s	120 s	10, 30, 70 s	60 s
P10, P11, P12	120 s	120 s	50 s	40, 80, 100 s

2.2. Characterization of coatings

The optical evaluation of the zinc coating was carried out with a secondary electron microscope (SEM). The SEM images were analysed three times with ImageJ to determine the degree of coating. Fig. 3 shows the principle of the ImageJ evaluation. Different grey scale values of deposited zinc (red) and non-coated aluminum (black) allowed the measurement of an arithmetic average of the surface coverage. The resulting zinc layer thickness was measured by incident light microscopy and glow discharge optical emission spectroscopy (GDEOS).

2.3. Casting setup and parameters

For casting experiments a hpdc unit DAK 450-54 (*Oskar Frech GmbH & Co. KG*) was used. After the insert was placed within the mold (Fig. 4a), both die halves were closed and pressed together with a maximum closing force of 458 tons. With a maximum plunger speed of 2, 3, 4 and 5 m/s melt was accelerated during form filling. Applying a vacuum system (*Fondarex® VACUPAC - MedioP*) to the mold, gas and solidification porosity was lowered to a level of <1%. Reduced shrinkage and porosity was achieved by using a dwell pressure of 750 bar. The casting tools were tempered at 190 °C.
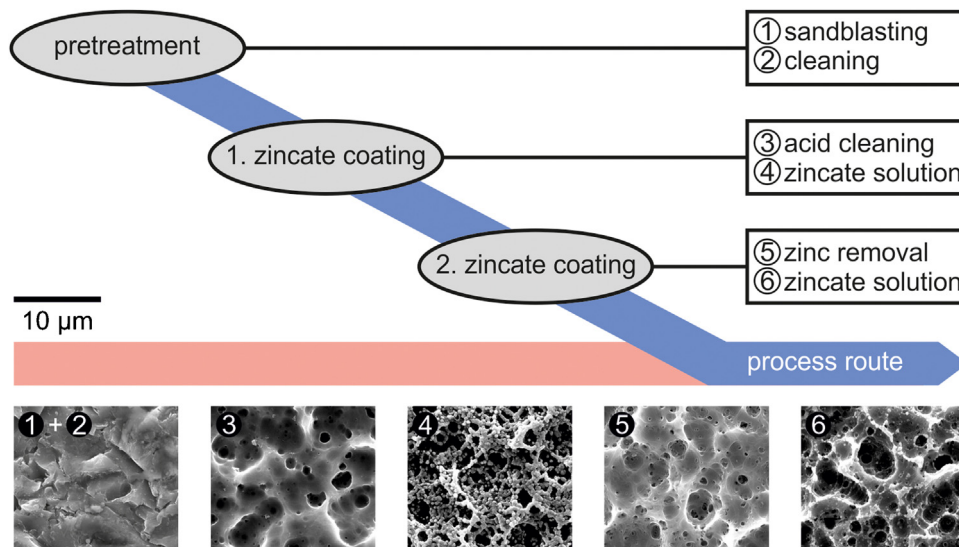

Fig. 2. Processing steps of zincate treatment and illustrating SEM-pictures of an AlMg3 coating sequence (parameter set AP).
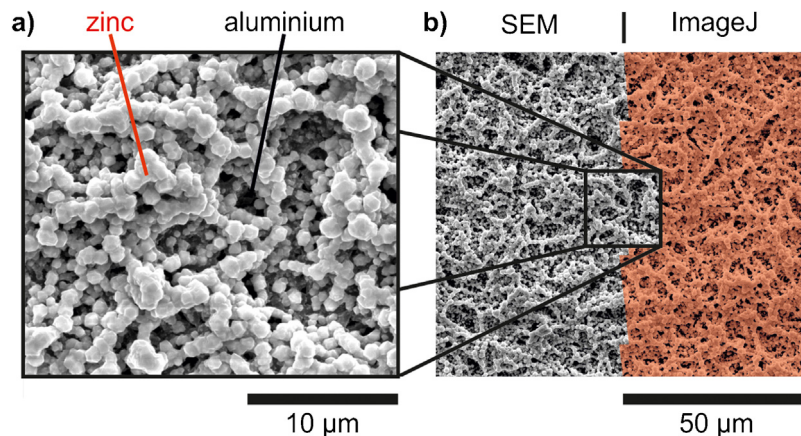

Fig. 3. Principle of the ImageJ measurements. (For interpretation of the references to colour in the text, the reader is referred to the web version of this article.)
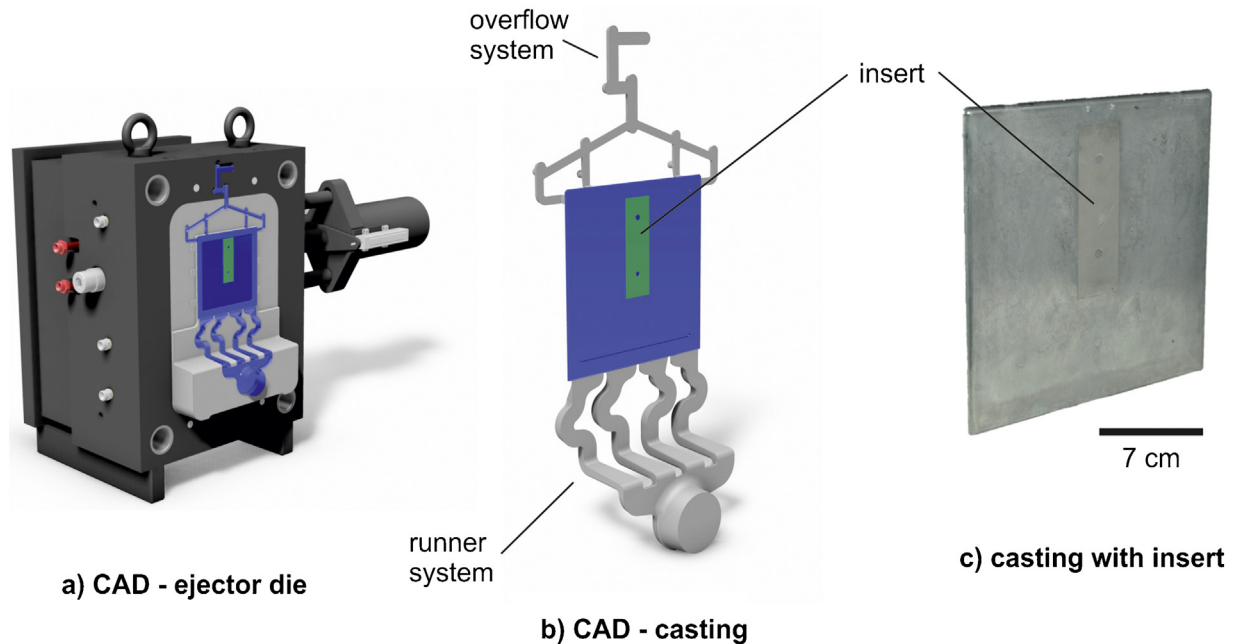
Fig. 4. Setup for casting experiments with a) CAD – ejector die half including the casting (blue) which is also given in CAD – detail b) Casting with runner and overflow system, c) compound casting. (For interpretation of the references to colour in this figure legend, the reader is referred to the web version of this article.)

In the presented work the die casting alloy 226D—AlSi9Cu3(Fe) was used and the initial melt temperature was set to a standard value of 740 °C and 680 °C for special experiments.

Prior to the casting cycle, aluminum inserts with dimensions of $100 \times 30 \times 1$ mm ($L \times W \times D$) including spacers made of expandable metals are placed vertically in the mold using fixing pins – see Fig. 4 green component. More information about the insert design can be found in Körner et al. (2014). The castings ($178 \times 178 \times 4$ mm) including the Zn-coated inserts are of a plate-like shape and constitute the basic sample design for further investigations – see Fig. 4c).

2.4. Analysis of Al–Al compound

For the metallographic preparation of the generated Zn coatings and the Al–Al-compounds the specimens were cut and embedded in cold-setting epoxy EpoFix (*Struers GmbH*). Microsections were grinded up to a grit of 2400. The subsequent polishing was carried out with a 3 μm diamond suspension. The analysis of the chemical composition at the Al–Al-interface was performed by EDX (EDAX) and microprobe analysis (*JEOL-JXA 8100*).

The compound strength was determined by compression shear tests. Samples with a dimension of $20 \times 8 \times 4$ mm ($L \times H \times D$) were tested for the different casting parameters. The tests were done in an Instron test machine at 0.2 mm/min, see Fig. 5a) or also Körner et al. (2014) for further information about the testing setup. The maximum shear strength τ_{max} was calculated according to Eq. (1).

$$\tau_{max} = F_{max}/A_{sample} \; \text{N/mm}^2. \tag{1}$$

For the alloys AlMg4.5Mn0.7 and AlMg3 τ_{max} was calculated after a cross head movement of 1 mm by dividing the force at break F_{max} through the interface area A_{sample} ($\approx 20 \times 8$ mm²). A minimum of five samples out of three castings was used. The tests were stopped after 1 mm because of plastic deformation which occurred for most of the applied wrought alloys at the insert section. In this stadium of deformation no layer delamination was detected. However shear strength values at the interface could be calculated for AlCu4MgSi samples. Due to their high strength (also see Fig. 1) and low plastic deformation, applied forces were transferred into the sample and

to the compound interface until the sample broke at the compound interface.

Fig. 5b) shows the experimental setup of the three point bending tests according to DIN EN ISO 7438. Samples with dimensions of $42 \times 20 \times 4$ mm ($L \times W \times H$) were tested. To evaluate the compound strength, the maximum force and the maximum movement distance of the cross head were determined. To complete the compound investigation break mechanism and fractured surfaces were analysed using SEM and EDX (*FEI*). Micro Vickers hardness measurements were carried out to gain information about the mechanical properties of the wrought alloys prior to and after hpdc casting – see Fig. 5c).

3. Results and discussion

3.1. Zincate treatment for Al wrought alloys

Fig. 6 shows SEM pictures of the wrought alloys with the best degree of coating in the presented setup and the corresponding dipping times. By comparing the three coated alloys it becomes clear that the zinc layer shows extremely different morphologies. This is due to two important facts: The dipping time and its consecutive reactions in the above listed chemicals (see Fig. 6) and the electromotive force (EMF)/electrochemical standard potential of the alloys. Wedler and Freund (2012) explained the basic effects of the EMF. Eq. (2) shows the correlation between the standard potentials of the alloying elements and the EMF. A positive value for ΔE^0 equals a high EMF and leads the reduction (ΔE^0_{red}) and oxidation (ΔE^0_{ox}) desired. Those standard potentials describe the driving force of the oxidation and reduction reactions in Eqs. (3) and (4). The higher the value, the lower the electronegativity and therefore less free electrons are produced.

$$\Delta E^0 = E^0_{red} - E^0_{ox} \tag{2}$$

The more positive the difference in Eq. (2), the greater the driving force of the reaction. A difference ΔE^0 at +0.900 V (see Table 3) results from oxidation of aluminum (E^0_{ox} – see Eq. (3)) and the
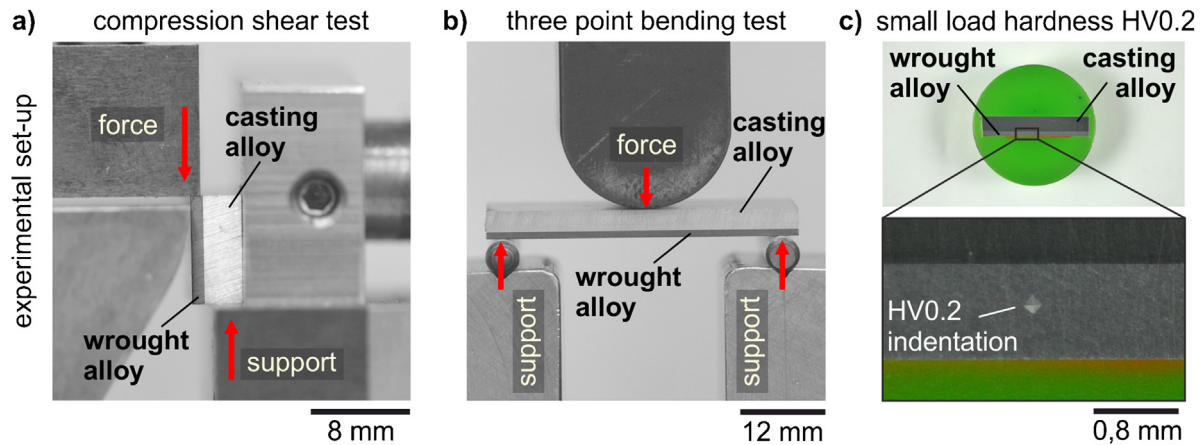
Fig. 5. Experimental setups of a) compression shear test, b) three point bending test and c) micro section sample for small load hardness test HV0.2.
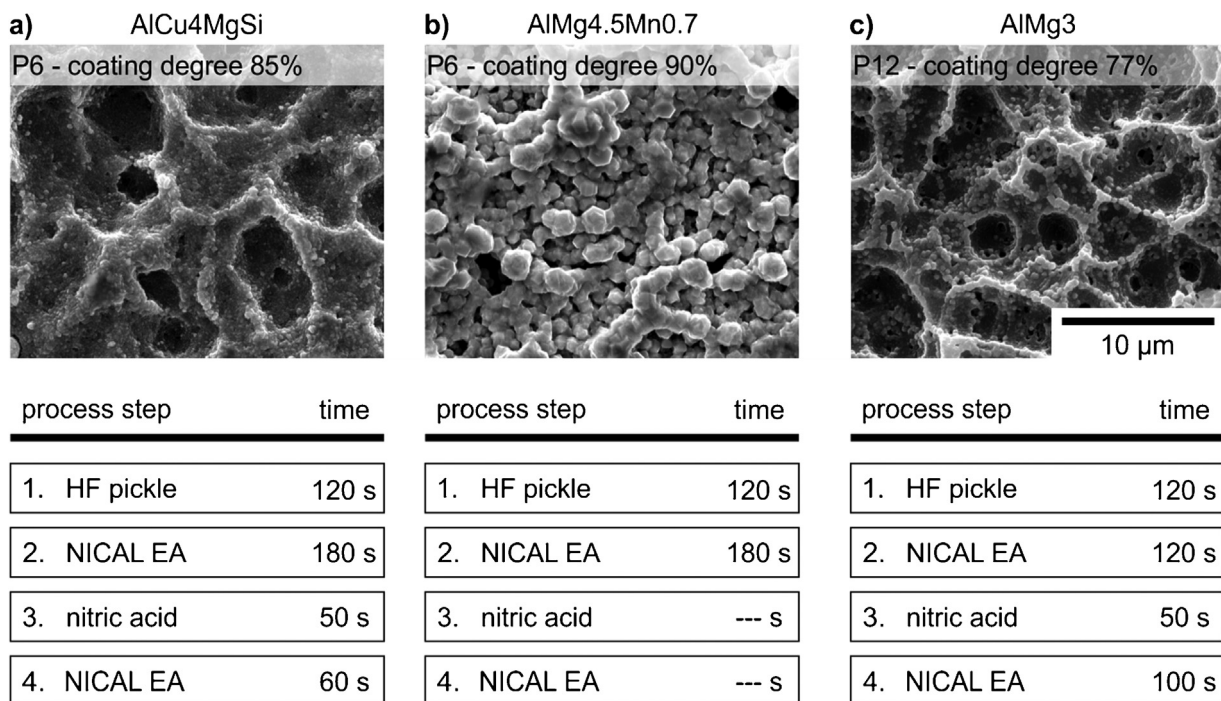

Fig. 6. SEM images of coated sheets. For each wrought alloy the coating parameters with the best degree of coating are shown.

Table 3
Selected elements and their reactions are part of the electromotive series, see also Wedler and Freund (2012).

Reaction	Standard potentials in ΔE^0
$Cu\|Cu^{2+}$	0.153
$Zn\|Zn^{2+}$	−0.762
$Mn\|Mn^{2+}$	−1.185
$Si\|Si^{4+}$	−1.240
$Al\|Al^{3+}$	−1.662
$Mg\|Mg^{2+}$	−2.372

reduction of zinc ($E^0{}_{red}$ – see Eq. (4)), which was confirmed by the theoretical investigations made by Jelinek (1997).

$$\text{Oxidation}: Al + 3OH^- \leftrightarrow Al(OH)_3 + 3e^- \tag{3}$$

$$\text{Reduction}: Zn^{2+} + 2e^- \leftrightarrow Zn \tag{4}$$
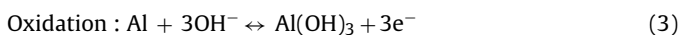
The reaction with magnesium actually results in a value for $\Delta E^0{}_{Mg/Zn}$ of +1.610 V and for copper $\Delta E^\circ{}_{Cu/Zn}$ is only −0.915 V with

zinc being the corresponding reduction agent. This means that the deposition is inhibited in aluminum-copper alloys. This correlates with the coating results in Fig. 6. AlCu4MgSi shows the smallest zinc crystals at the surface, and for AlMg4.5Mn0.7 being the corresponding insert material with the highest magnesium concentration, even a single zincate step is sufficient to get satisfying coating results.

Fig. 7 shows the results of the GDOES measurements. The aluminum-copper alloy exhibits the thinnest zinc layer. An increase in the magnesium content promotes the growth of the layer thickness, which is also caused by the EMF and correlates with the results of the coating degrees (see Fig. 6). Measuring an actual layer thickness based on GDOES measurements is not possible because selective etching is observed over the whole sample. Nevertheless, those investigations allow comparative studies between the coated alloys and support the statement that coating thicknesses produced by means of zincate coating are less than 1 μm. In the present work coatings for AlMg4.5Mn0.7 are the exception, because instead of double zincating the alloy, a simple zincate step was chosen to
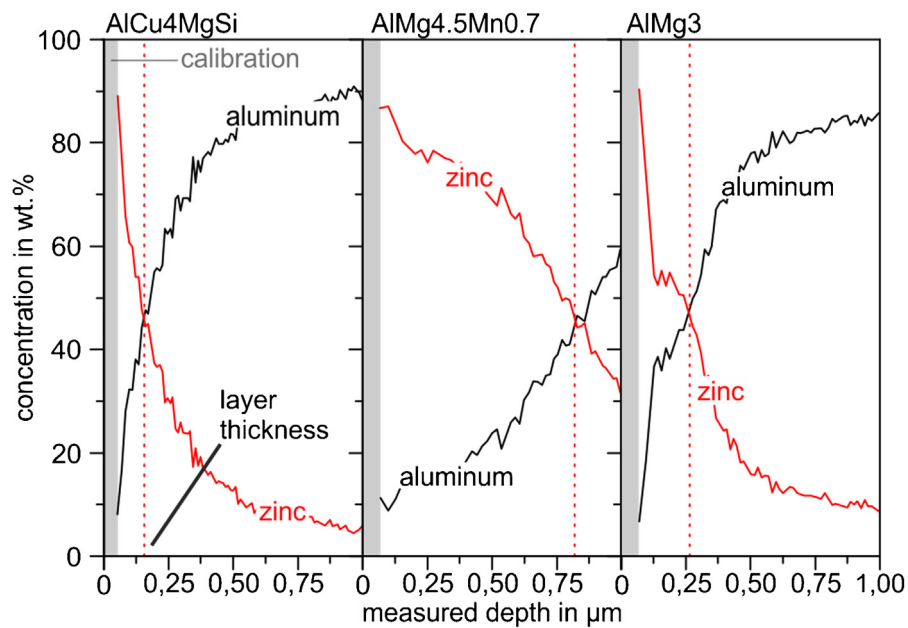
Fig. 7. GDOES depth profile of the integrated wrought alloys after the zincate process.

reduce coating times. Hence, a thicker layer of zinc is observed and correlates with the zincate parameter studies performed by Hino et al. (2009) and theoretical approaches of Jelinek (1997).

3.2. Al–Al compounds

3.2.1. Influence of the casting parameters

The samples were produced at different crucible temperatures (680 °C and 740 °C) and plunger velocities of 2 m/s and 5 m/s. The investigations of the influence of casting parameters on the interface were performed by microprobe measurements. Fig. 8 shows the results of the microprobe measurements of AlCu4MgSi and AlMg4.5Mn0.7 in the as-cast state and after a heat treatment for 1 h at 370 °C. In the microprobe pictures it becomes obvious that the zinc concentration depends mainly on the coating parameter and on the chosen wrought alloy. The zinc diffuses mainly into the casting alloy. There is no evidence that crucible temperature and plunger velocity have any influence on the diffusion depth. A great opportunity emerges from the images of specimens with T4-heat treatment (1 h – 370 °C) – Fig. 8. A high solubility of zinc in aluminum allows an exact adjustment of the zinc concentration at the interface between the alloys. Thus, it is possible to produce a homogenous joining area between the casting and the wrought alloy. It would be expected that such a heat treatment could improve the bonding properties at the interface of the compound casting because mechanical interface properties are no longer dominated by elementary zinc and its poor mechanical values compared to aluminum alloys.

3.2.2. Mechanical properties

Measurements are taken from castings which were produced at $T_{crucible} = 740$ °C and $v_{plunger} = 2$ m/s. The results for the maximum shear strength strongly depend on the wrought alloy. AlCu4MgSi achieved an average shear strength of 61.8 MPa ± 7.4 MPa. The shear strength of the alloys with magnesium as main alloying element was determined to be a lot lower than alloys rich in copper. AlMg4.5Mn0.7 reached a mean value of 54.4 MPa ± 2.0 MPa, whereas AlMg3 showed a mean shear strength of 40 MPa ± 0.7 MPa.

The experimental setup in Fig. 9 demonstrates the reason for the differences in the measured shear strengths. The wrought alloys AlMg3 and AlMg4.5Mn0.7 showed massive plastic deformation in the force input zone during the experiment, see Fig. 9a). This plastic deformation was the reason why the experiments were stopped after a cross head movement of 1 mm. The differences within the measured values are of the same magnitude as the yield strengths of the tested alloys. This fact allows the conclusion that the interface stability is greater than the yield strength of the wrought alloys of AlMg3 and AlMg4.5Mn0.7 for this experimental setup.

As can be seen in Fig. 9b) and c) for AlCu4MgSi compound castings only negligible plastic deformation could be detected. Yet, in this setup the shear mechanism is not solely a 2D effect due to possible sample inclinations. Fig. 10a) shows the results of the compression shear tests for AlCuMgSi, produced at different plunger velocities at a crucible temperature of 740 °C. Literature states a shear strength of 262 MPa for AlCu4MgSi, which was not achieved for compound samples (max. 69 MPa). Within the parameter study of plunger velocity the deviation leads to the assumption that the melt velocity does not influence the formation of metallic bonding during casting. Yet, a high degree of metallic bonding must be accomplished due to the high reproducibility of the shear strength values. Finally, shear strength measurements clearly demonstrate, that the interface strength – determined by zinc – is the weakest part of the compound castings.

The different compound casting samples were tested by means of three point bending tests. An influence of the casting parameters, like crucible temperature and plunger velocity could not be detected. It appears that the mechanical properties of the castings could be improved by using different composite materials. Fig. 10b) depicts forces at the point of catastrophic failure in comparison to small load hardness values of the wrought alloys prior to and after casting. The plot shows the results of the casting series at a constant crucible temperature of 740 °C and a plunger velocity of 2 m/s. Results indicate that using high-strength wrought alloys can increase the maximum force which is applied on the specimens. The compound based on AlMg4.5Mn0.7 and AlMg3 nearly achieved the level of the pure casting alloy AlSi9Cu3(Fe). The maximum force which can be applied to the AlCu4MgSi-based compound is even about 1 kN higher compared to the pure casting alloy. This observation can be explained by the high strength of the wrought alloy. In regions of tensile stresses it prevents crack initiation and -propagation.
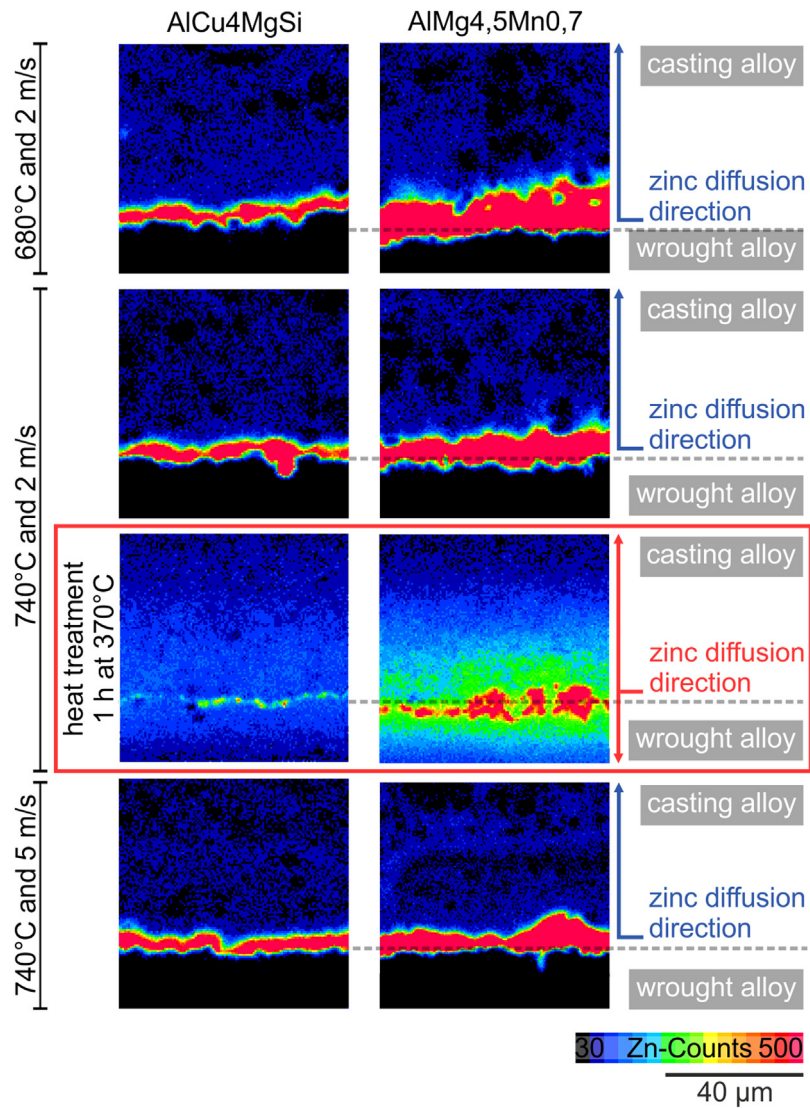
Fig. 8. Microprobe measurements of AlMg4.5Mn0.7 and AlCu4MgSi for varying casting and heat treatment parameters. Due to scattering effects Zn-layers appear much thicker than they actually are (<1 μm) – see also GDOES-measurements in Fig. 7.
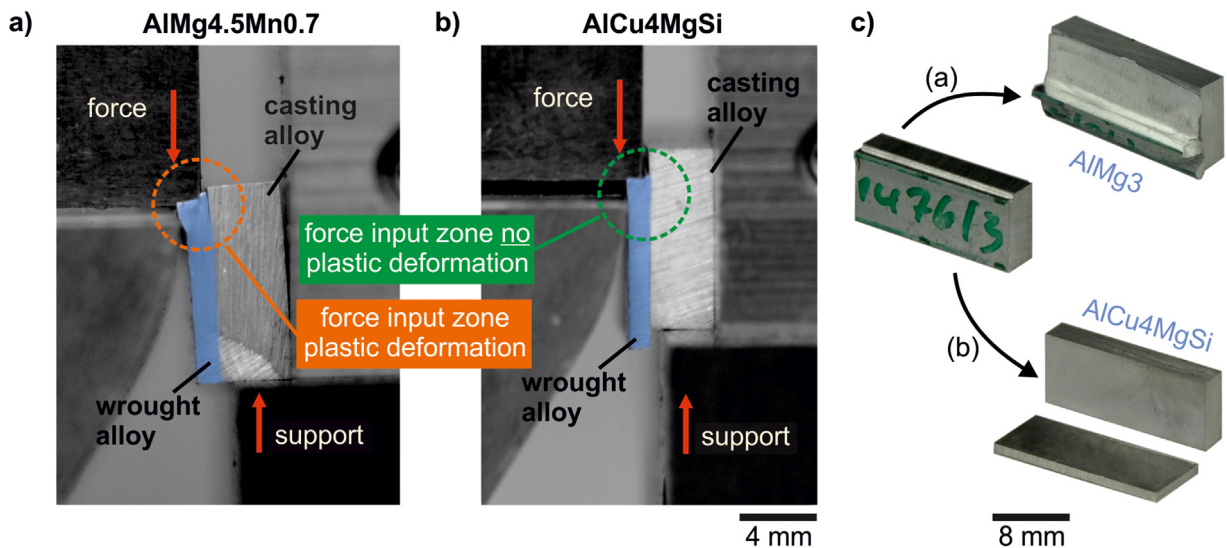

Fig. 9. Failure behavior druing the compression shear test. a) AlMg4.5Mn0.7 compound with no visible plastic deformation. b) AlCu4MgSi compound for high strength wrought alloys. c) Samples after testing.
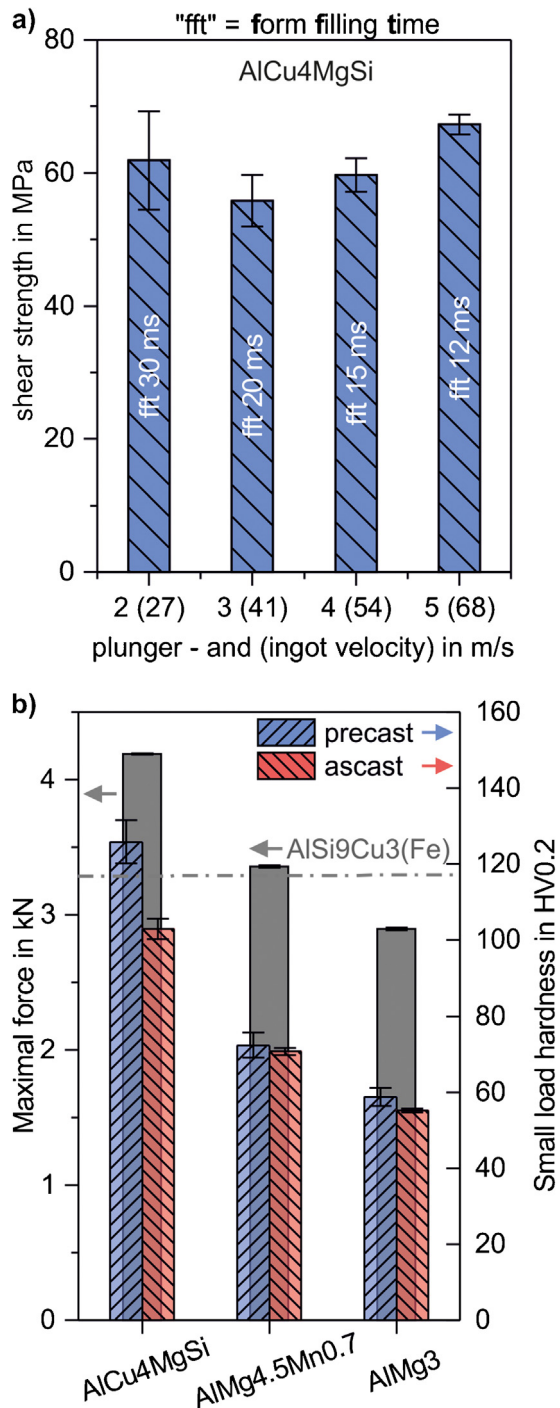
Fig. 10. Results of mechanical tests. a) shear values of AlCu4MgSi-based compound structures and b) 3-point-bending test depicted together with small load hardness values prior to and after casting.

On the one hand small load hardness values in Fig. 10b) show that wrought alloys based on magnesium as main alloying element keep their mechanical strength although the casting process itself represents a heat treatment for the sheet material. This is due to the solid solution hardening effect of this group of alloys which seems to be completely unaffected by production time and melt temperature for one casting. AlCu4MgSi is losing some of its hardness (about 20 HV0.2) compared to the precast state, which might be due to recovery effects or a coarsening of its hardening phase. According to Kammer (1998), precipitation strengthening is the main hardening effect based on Cu-rich, semi-coherent (GP-

II + θ")-zones for this group of alloys. Being a non-equilibrium phase a thermal treatment for the time range of a casting shot is enough to partially transform the hardening phase to its next stable form in the precipitation sequence. The transformation from GP-II + θ" to θ' involves a loss of coherence and therefore the strengthening effect of the precipitation is reduced as shown in Fig. 10b) for AlCu4MgSi. Nevertheless a strengthening effect for compound castings with incorporated AlCu4MgSi sheets is observed and the bearable load at break is increased by 19.8% compared to pure AlSi9Cu3 samples. The mechanical tests show that very good interface conditions and compound properties can be achieved by the presented coating and casting setup.

3.2.3. Fracture surface analysis

As shown in Fig. 9c) sudden delamination takes place at the end of pressure shear tests with AlCu4MgSi-based compounds. The main failure mechanism is observed to be a combination of ductile fracture and forced fracture – see Fig. 11.

At the start of the testing procedure forces are introduced in the upper part of the shear sample. Elastic deformation in the wrought alloy leads to a ductile fracture in the upper part. Therefore the effective load-bearing area is reduced, yet applied forces are rising until the maximum shear strength is reached. At this stadium of the test wrought as well as cast alloys behave rigid without forming ductile interfaces and therefore the rest of the interface shows a fracture surface according to sudden forced rupture mechanism. Again, this confirms that the shear test setup is not fully 2D because the applied force interacts not simultaneously with the whole interface area.

Fig. 12 shows SEM-pictures of a fractured surface with a different mechanism. A primary and secondary fracture surface is identified but is located independently of the applied stress direction. EDX measurements indicate a much higher oxygen content (ca. 30%—oxygen) on the surface of the aluminum wrought alloy in the primary fracture area than for the secondary fracture area (ca. 3%—oxygen).

Therefore it is highly likely that oxidation took place prior to or during casting, reoxidation due to altered chemical baths being one possibility. Considering only EDX measurements it is not possible to gain information about which oxide has been formed. Nonetheless it is obvious that oxidation prevents sufficient wetting with aluminum melt and the formation of a metallic bonding. Samples with obvious oxidation were detected for very few castings and thus have not been taken into consideration for the shear strength measurements, as shown in Fig. 10.

4. Conclusions

Applying very thin zinc coatings is a successful approach to create sound metallic compound castings. The main findings can be stated as followes:

- The zincate treatment technology leads to sound metallic bonds without the formation of brittle intermetallic phases. This effect mainly refers to the high solubility of Zn in Al-solid solution and the low overall Zn content introduced by zincate technology.
- There is a minor influence of casting parameters on interface/compound properties. Within the process window for reasonable high pressure casting parameters time and temperature values are too narrow to actually make a difference.
- Due to the different electrochemical potential of the wrought alloy and its alloying elements the zincate treatment has to be adapted to different insert alloys. The higher the potential of the elements, the longer is the coating time for the insert and the
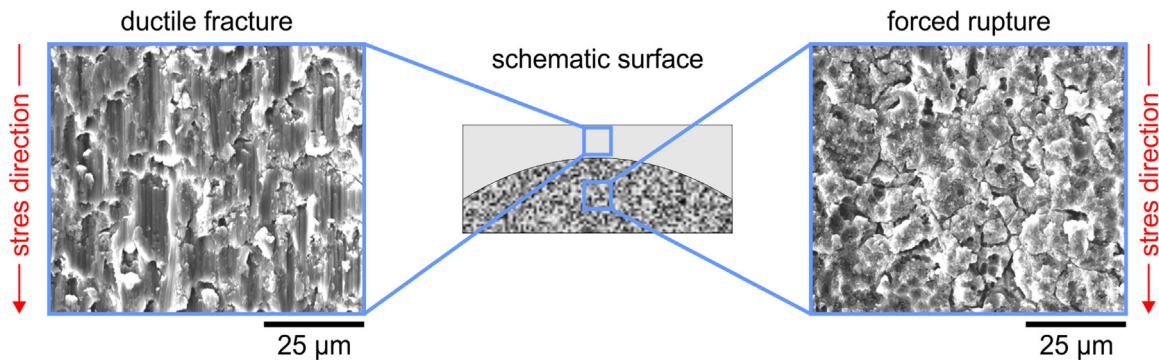
Fig. 11. Failure mechanism for pressure shear tests (AlCu4MgSi + AlSi9Cu3). SEM-images of fractured surface at wrought alloy segment.
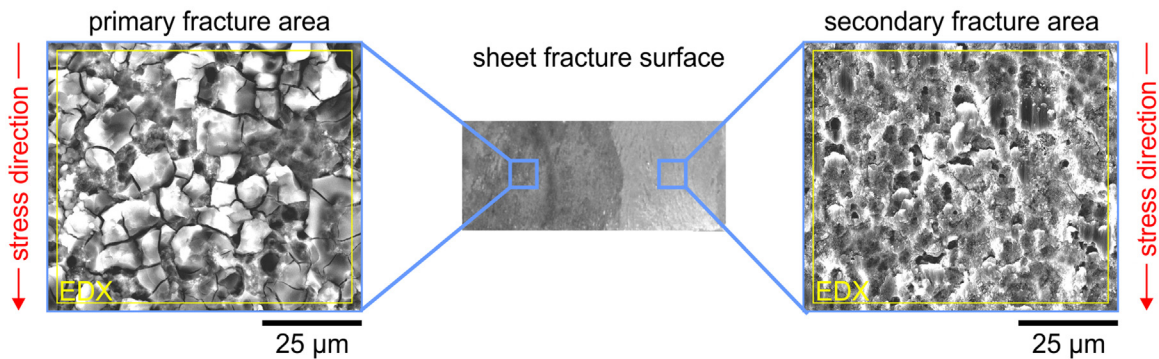

Fig. 12. SEM-images of a fractured surface (Al wrought sheet side).

smaller are the Zn crystals, which can be explained by a reduced driving force to actually deposit Zn.

- The mechanical properties of Al–Al-compound castings can exceed those of monolithic castings. Especially the 3-point-bending test demonstrates clearly that integrating an aluminum wrought alloy component in the right position (e.g. region of tensile stresses) can lead to enhanced mechanical properties.
- Heat treatment is a promising approach to enhance compound properties and create compounds with an interface characterized by a smooth and widened distribution of alloying elements. Again, this addresses the high solubility of Zn in Al solid solution. It has also to be stated though that Fe, which apparently is codeposited during zincate treatment, remains at the compound interface and cannot be distributed during the heat treatment in the same manner as Zn.

Acknowledgements

References

DIN EN 1011-4, Welding – Recommendations for welding of metallic materials – Part 4: Arc welding of aluminum and aluminum alloys.

DIN EN 573-3/4, Aluminum and aluminium alloys – chemical composition and design of semi-finished products.

DIN EN ISO 7438, Metallic materials – Bend test.

DIN ISO 8486-2, Bonded abrasives – Determination and designation of grain size distribution – Part 2: Microgritzs F230–F2000 (ISO 8486-2:2007).

Hino, M., Murakami, K., Mitooka, Y., Muraoka, K., Furukawa, R., Kanadani, T., 2009. Ni-P coating onto various aluminum alloys. Mater. Trans. JIM 50, 2235–2241, http://dx.doi.org/10.2320/matertrans.L-M2009819.

Jelinek, T.W., 1997. Oberflächenbehandlung von Aluminium. Eugen G. Leuze Verlag, Saulgau, ISBN 3874801152.

Jin, J.G., Lee, S.K., Kim, Y.H., 2004. Adhesion improvement of electroless plated Ni layer by ultrasonic agitation during zincating process. Thin Solid Films 466, 272–278, http://dx.doi.org/10.1016/j.tsf.2004.02.100.

Körner, C., Schwankl, M., Himmler, D., 2014. Aluminum–aluminum compound castings by electroless deposited zinc layers. J. Mater. Process. Technol. 214, 1094–1101, http://dx.doi.org/10.1016/j.jmatprotec.2013.12.014.

Kammer, C., 1998. Aluminium-Taschenbuch, fifteenth ed. Aluminium-Verlag, Düsseldorf, ISBN-10: 3810172428.

Liu, T., Wang, Q., Sui, Y., Wang, Q., Ding, W., 2015. An investigation into aluminum–aluminum bimetal fabrication by squeeze casting. Mater. Des. 68, 8–17, http://dx.doi.org/10.1016/j.matdes.2014.11.051.

Ostermann, F., 2007. Anwendungstechnologie Aluminium, second ed. Springer, Berlin, ISBN-10: 3540238824.

Papis, K.J.M., Hallstedt, B., Löffler, J.F., Uggowitzer, P.J., 2008. Interface formation in aluminium–aluminium compound casting. Acta Mater. 56, 3036–3043.

Papis, K.J.M., 2009. Processing Strategies in Light Metal Compound Casting, Dissertation. ETH Zürich, Zürich.

Rübner, M., Körner, C., Singer, R.F., 2011. Aluminium–aluminium compound fabrication by high pressure die casting. Mater. Sci. Eng. A 56, 170–175, http://dx.doi.org/10.1016/j.msea.2011.05.076.

Schwankl, M., Kellner, R., Singer, R.F., Körner, C., 2013. The influence of sandblasting on the morphology of electroless deposited zinclayers on aluminum sheets. Appl. Surf. Sci. 283, 202–208, http://dx.doi.org/10.1016/j.apsusc.2013.06.082.

Viala, J.C., Peronnet, M., Barbeau, F., Bosselet, F., Bouix, J., 2002. Interface chemistry in aluminium alloy castings reinforced with iron base inserts. Composites Part A 33, 1417–1420.

Wedler, G., Freund, H.J., 2012. Lehrbuch der Physikalischen Chemie. Wiley-VCH Verlag, Weinheim.

Zhang, H., Chen, Y., Luo, A.A., 2014. A novel aluminum surface treatment for improved bonding in magnesium/aluminum bimetallic castings. Scr. Mater. 86, 52–55, http://dx.doi.org/10.1016/j.scriptamat.2014.05.007.